Insulator-based Dielectrophoretic Lab-on-a-Chip System for Erythrocytes

Soumya S. Keshavamurthy, Mississippi State University, Mississippi State, MS, USA
Shirley Anell Pullen, Mississippi State University, Mississippi State, MS, USA
Adrienne R. Minerick, Mississippi State University, Mississippi State, MS, USA

Abstract

Medical lab work, such as blood testing, will soon be near instantaneous and inexpensive via capabilities enabled by the fast growing world of microtechnology. Previous research by the authors has shown that erythrocytes of different blood types respond differently in AC dielectrophoretic fields. These results suggest that spatial separation in the electric field depends on the blood type antigen expressed on the surface of the erythrocytes. This attribute forms the foundation for the continuous flow, DC dielectrophoretic research presented here. In this work, no electrodes are placed within the microchannel, thus simplifying fabrication and reducing electrode/cell interactions. Instead, a DC electric field is applied remotely and an insulating obstacle in the microfluidic channel creates a spatially non-uniform electric field. In our work, we utilize PDMS obstacles of rectangular, trapezium and semi-circle geometrical configurations on the order of 100 μm in breadth. Device dimensions were optimized by evaluating the behaviors of fluorescent polystyrene particles of three different sizes roughly corresponding to the three main components of blood: platelets (2-4 μm), erythrocytes (6-8 μm) and leukocytes (10-15 μm). This work provides the operating conditions for which size dependent blood cell DC dielectrophoresis can be performed. The optimized device is being used for continuous separation of erythrocytes. The design enables collection into specific channels based on the cell's deflection from the high field density region of the obstacle. By monitoring cell accumulation in the outlet ports, we expect to be able to infer blood type for unknown samples of blood. If successful, this developed technique can be directly applied for use in portable blood diagnostic devices for easy, accurate and rapid analysis.

Introduction

Lab-on-a-chip systems have the capacity to perform a variety of tasks ranging from DNA analysis to protein recognition and can also be catered to point-of-care medical diagnostic tools. Lab-on-a-chip (LOC) devices integrate multiple laboratory functions on a single square centimeter chip and are capable of handling extremely small fluid volumes down to picoliters [1-4]. They commonly utilize electrokinetics to move analytes because electric fields are versatile and can be precisely controlled for specific, quantifiable analyte responses. Furthermore, devices employing electric fields can eventually be simplified to only require a battery for power – a key characteristic for true portable diagnostic devices. One type of electrokinetics, dielectrophoresis (DEP), uses spatially non-uniform alternating current (AC) electric fields, which controls particles or cells through transient polarizations. Dielectrophoresis is a key type of field to explore in medical diagnostic devices due to operational simplicity, requirement of lower voltages, and small sample volumes all of which enable device portability [2].

Direct Current dielectrophoresis (DC-DEP) or insulator-based dielectrophoresis (iDEP) is a relatively new field. It utilizes the spatially nonuniform electric field component but not the frequency dependent component of dielectrophoresis, which has been shown to be adequate for manipulation of cells [5]. Spatial non-uniformities in the electric field are generated via insulating obstacles positioned in microdevice channels through which a DC current is passed. The advantages of using insulating obstacles include [6]:

1. Insulators are less prone to fouling than electrodes embedded in microdevices,

2. No metal components are involved which reduces the complexity of fabrication of devices,
3. Ideal insulating obstacles are mechanically robust and chemically inert, and
4. Electrolysis gas evolution at the remotely located metal electrodes does not result in bubbles inside the channel.

Initial work on iDEP was conducted by Cummings and Singh in 2003. Their configuration contained an array of insulating posts where two operating regimes were observed, namely streaming and trapping DEP [7]. In streaming DEP, particles concentrated at electric field maxima, travel down in flowing streams, and in trapping DEP the forces reversibly immobilize the particles on the insulating posts. Subsequently, Lapizco-Encinas *et al.* used insulating posts to concentrate and sort live and dead *E.coli* [5] where live cells exhibited trapping DEP and dead cells exhibited streaming DEP. They also demonstrated that dead cells exhibited less negative DEP compared to live cells. In these cases, size was maintained constant while cell properties varied. There were many efforts to explore other insulating materials for iDEP included cyclo-olefin polymers by Mela *et al.* in 2005 [8], and an oil droplet obstacle [9] in 2006. Thwar *et al.* (2007) demonstrated dielectrophoretic potential wells using pairs of insulating oil menisci to shape the DC electric field [10] and Zhang *et al.* simulated and modeled separation in a circular channel [11]. Fabrication of these microdevices have been achieved using silica or glass, thermal plastics such as polymethylmethacrylate (PMMA), polyolefins, polyethylene terephthalate, and polycarbonate or elastomers such as poly(dimethylsiloxane) (PDMS) [12]. A number of insulating obstacles have been explored by other researchers that comprise different shapes like rectangle [13], triangle [13], circular [12] and saw-tooth [14]. A complete picture of shape and voltage dependencies in those devices has not yet been attained.

This paper discusses a novel premise of using DC dielectrophoresis to ascertain cell behaviors for the blood types of the ABO system (A^+, B^+, AB^+, O^+, A^-, B^-, AB^-, and O^-). Previous research by the authors has shown that blood types respond differently in AC dielectrophoretic fields. Dielectrophoretic movement for the red blood cells followed distinct trends with time for each blood type and was quantified by these parameters: total cell count, vertical movement, horizontal movement, and distance. All parameters at 95% confidence interval revealed that type O^+ was easily distinguishable from the other blood types with types A^+ and B^+ having similar responses in the dielectrophoretic field. Blood type A^+ deflects from high field density region followed by type B^+ and AB^+, whereas type O^+ displays small deflections in the nonuniform 1 MHz electric field with 0.025 V_{pp}/μm strength [3]. These observed cell blood type deflections have been attributed to the functionalized ABO antigens on cell membranes [3]. These results suggest that spatial separation in the electric field depends on the blood type antigen expressed on the surface of the erythrocytes.

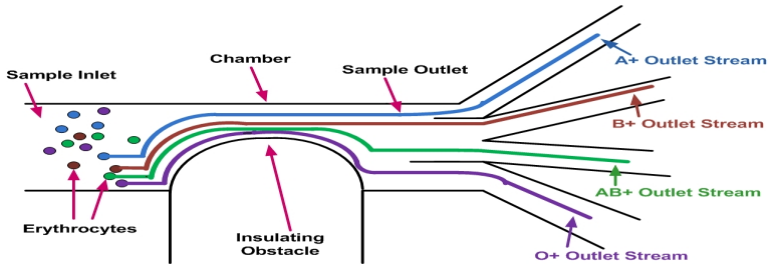

Figure 1: Insulating obstacle in a channel followed by channel bifurcations for sorting.

This attribute forms the foundation for the continuous flow, DC dielectrophoretic research outlined here. In DC-DEP, successful separation of cells into outlet channels is dependent on the deflection from the insulating obstacle (Figure 1). The preferred blood type channel is hypothesized from AC-DEP erythrocyte response results from previous research [3]. Cell accumulation at the outlet channel end ports will correspond to a specific blood type.

PDMS obstacles of varying geometrical configurations (rectangle, trapezium, and semi-circle) were utilized to create a spatially non-uniform electric field and blood types (A^+, B^+, AB^+, O^+, A^-, B^-, AB^-, and O^-) will be tested as they age (day 0, 1, 3 and 5). Results on fabrication and dependency studies: polystyrene experiments for size dependency, dilution experiments and optimizing the device design and selection of specific obstacle geometry have been presented here. Future goals are to fabricate microdevices with new optimized design parameters and again test for size dependency (fluorescent polystyrene particles) and antigen expression (red blood cell) dependency. This developed technique can be directly applied for use in portable blood diagnostic devices for easy, accurate and rapid analysis. Dielectrophoretic characterizations in lab-on-a-chip devices would be far more portable than current assay techniques.

Theory

In DC dielectrophoresis, an insulating obstacle is utilized to create a spatially non-uniform electric field. The movement of the particle in the electric field gradient is due to the resulting dielectrophoretic force acting on the polarizable particle [1, 2, 15]. The non-uniform field force can be derived from the net dielectric force as shown:

$$F = (p \cdot \nabla) E \tag{1}$$

where 'p' is the dipole moment vector which is a function of particle's effective polarizability, 'α', volume, 'v', of the particle and the applied electric field, 'E' as shown:

$$p = \alpha v E \tag{2}$$

The Claussius-Mossotti factor, α estimates the effective polarizability term of the particle and is a ratio of complex permittivities $\tilde{\varepsilon}$

$$\tilde{\varepsilon} = \varepsilon - i\sigma/\omega \tag{3}$$

where 'ω' represents frequency, 'ε' the dielectric constant and 'σ' the electrical conductivity of the medium. There is no frequency component involved in DC-DEP and the dielectrophoretic force is estimated to be the residual of Claussius-Mossotti factor when the limit of the frequency approaches zero. This simplification is substituted into the dielectrophoretic field force equation:

$$F_{DEP} = \frac{1}{2} v \frac{\sigma_p - \sigma_m}{\sigma_p + 2\sigma_m} \nabla E^2 \tag{4}$$

A spatially dense non-uniform field is created around the obstacle as the DC field lines diverge around the insulator. Due to the insulating obstacle, a high electric field density region is produced between the obstacle and the channel wall which aids in particle motion. Since DC-DEP forces push the particle towards or away from the high field density regions, the particle experiences an attractive or repulsive force as it flows around the corner of the obstacle, thus facilitating particle motion according to its polarizability. Many geometrical configurations and operating conditions are possible as a result of DC dielectrophoresis. In this

work, a DC electric field is used to generate a field inside a channel, but around a rectangle, trapezium and semi-circle obstacle. Two dependencies are studied: size dependency using fluorescent polystyrene particles and antigen dependency using red blood cells of each blood type.

Materials and Methods

Variables in this research are: voltage of the DC source, device geometry, fluorescent polystyrene particles, blood type, and time of blood storage. Blood samples will be analyzed in the dielectrophoretic field on day 0 (day of donation), 1, 3 and 5 in storage at 5^{o}C. The important steps in the process are device design, microdevice fabrication by soft lithography, experimentation (including microsample preparation), image analysis and quantification via total cells in each outlet channel. Each of these steps is discussed below:

Red Blood Cells (RBC) / Erythrocytes

They are biconcave in shape to maximize surface area for gas (O_2 and CO_2) transport across their membrane. Their diameters range between 6 to 8 microns with changes in response to solvent conditions, pH and temperature. RBC's have a net negative charge based on their conventional linear electrophoretic behavior [16] with their outer membrane being nonconductive ($\sigma \leq 1$ μS/m) [17] and the interior being conductive (σ = 0.53 to 0.31 S/m) [18]. Human blood types are classified based on (1) membrane surface antigens that span the entire membrane and (2) blood plasma antibodies [16]. Type A blood expresses antigen A, Type B blood expresses antigen B, Type AB blood has both A and B antigens while Type O blood has neither antigens [16]. The A and B antigen differ by side chain modifications. The A antigen terminates in an α 1,3 – linked N-acetylgalactosamine while B terminates in an α 1,3 – linked galactose. The presence or absence of the Rhesus (Rh) factor antigen determines the positive (present) and negative (absent) blood types [19]. The 8 ABO / Rh blood types are A^+, B^+, AB^+, O^+, A^-, B^-, AB^-, and O^-.

Device Design

AutoCAD software (Autodesk, Inc) was used to design the microdevice mask, which was printed on transparencies with a resolution of 32,512 dpi (Fine-Line Imaging, Inc.). The device consists of one inlet (200 μm wide) and 4 outlet channels (100 μm wide). The distance between the inlet and outlet ports was 4.5 cm. An insulating obstacle of varying geometry was positioned in the inlet channel at a distance of 150 μm upstream from the bifurcation to the four outlet channels. The obstacle geometries (rectangle, trapezium and semi-circle) are shown in Figure 2 (a), (b) and (c) with the complete microdevice design shown in Figure 2 (d).

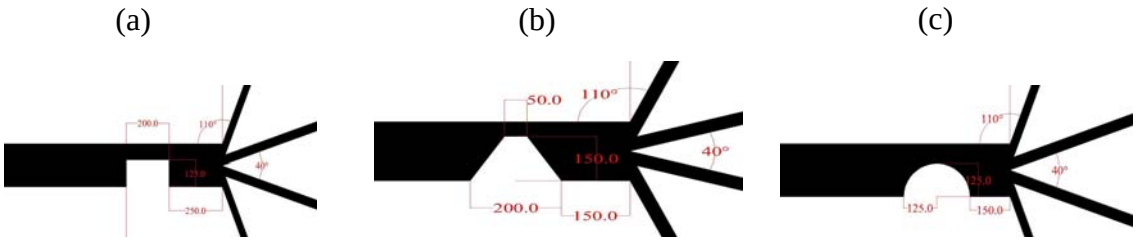

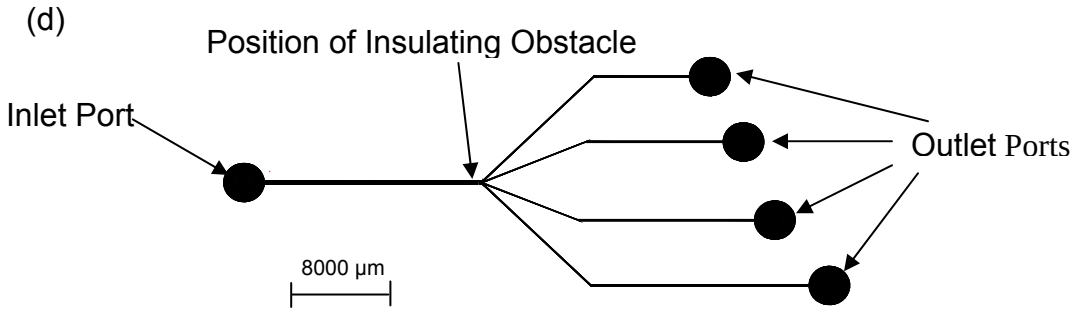

Figure 2: Insulating obstacle geometries and microdevice with inlet and outlet channels (a) Rectangular Obstacle Geometry (b) Trapezium Obstacle Geometry (c) Semi-Circle Obstacle Geometry (d) Microdevice design with inlet and outlet channel ports

Fabrication

The device was fabricated with a sample injection port and four outlet ports. This microdevice consisted of a glass slide and lithographically patterned microchannel of poly(dimethylsiloxane) (PDMS). Standard techniques of soft lithography were used to pattern the microdevice [12]. Some modifications in the process included employing UV-Ozone (UVO) cleaning procedure before SU-8 negative photoresist coating on the wafer, increasing the exposure time with the masked UV light and soft / hard bake temperatures and times. Figure 3 shows the patterned silicon wafer for different obstacle geometry. For the rectangular obstacle geometry, the inlet channel width of the patterned master (silicon wafer) increased by 20% compared to the mask dimensions, the width of the obstacle decreased by 11%, the distance between the obstacle and the channel wall increased by 13%, and the distance from the obstacle to the bifurcation point matched with that of the mask. For trapezium and semi-circle obstacle geometries, the width of inlet channel increased by 14%, width of obstacle decreased by 18%, distance between channel wall and the obstacle increased by 50% and the distance from obstacle to bifurcation point decreased by 22%.

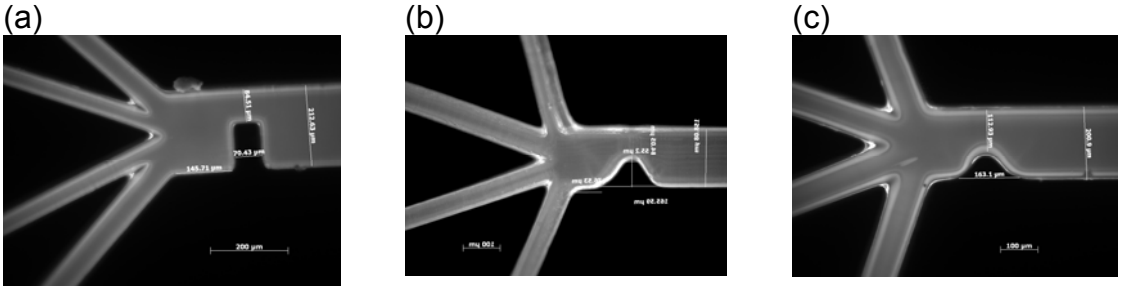

Figure 3: Patterned silicon wafer with rectangle, trapezium and semi-circle insulating obstacles. (a) Rectangular Obstacle Geometry (b) Trapezium Obstacle Geometry (c) Semi-Circle Obstacle Geometry.

PDMS was used to produce the microdevice from the patterned silicon wafer. Dow Chemical's Sylgard 184 pre-polymer base and curing agent were mixed in the ratio of 10:1, degassed for 15 minutes inside a vacuum chamber to remove suspended bubbles and poured onto the patterned negative relief silicon wafer. This wafer-PDMS assembly was cured in a 65^{o}C oven for 12 hrs. The PDMS layer was peeled from the patterned silicon wafer and sealed onto a glass slide using UVO treatments. Biopsy punches were used to create inlet and outlet

ports of 3 mm in diameters. Electrodes were positioned in the inlet and outlet ports and then connected to DC power supply. Figure 4 shows the PDMS microdevice on a glass slide with electrodes in the ports.

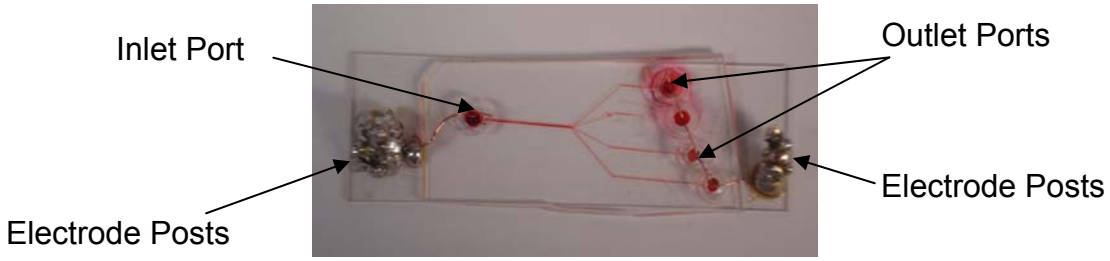

Figure 4: Typical PDMS microdevice sealed to a glass slide with electric connections and red food color in the channels for contrast.

Operation

DC dielectrophoretic force acting on a particle is proportional to its volume and subsequently size [5]. Therefore, two dependencies are simultaneously explored in this work: red blood cell type and blood cell size. This is possible because blood type antigens are expressed only on the red blood cells (erythrocytes) while whole blood is comprised of three different cells ranging in size from 2 μm (platelets), 7 μm (erythrocytes), and 11 μm (leukocytes). All work was conducted in a certified Biosafety Level II laboratory (BSL II) with Institutional Biosafety Committee (IBC) and Institute Review Board (IRB) for human subject's approval.

Polystyrene Particle Experiments

Fluorescent polystyrene particles (Bangs Laboratory, Inc) of three different diameters 2.28 μm (yellow, 540 or 600 nm emission), 5.49 μm (red, 660 or 690 nm emission) and 10.35 μm (green, 480 or 520 nm emission) were selected to roughly correspond to platelets, erythrocytes and leukocytes respectively. These particles were tested as a size dependence reference and will be compared against the separation and collection of actual blood cells into different channels in the microdevice shown in Figure 4. Based on the separation of these particles in all the three designs and the ease of fabrication, single obstacle geometry of rectangle was selected for further analyzing the blood samples. Individual as well as mixtures of all three sizes of polystyrene particles were used for experiments. Fluorescent polystyrene particles were diluted to 1:100 with 0.14M phosphate buffer saline (PBS) and introduced into the device through the inlet port for individual polystyrene experiments. A DC power supply was used to deliver a voltage of 5 V (field strength of 1.11 V_{pp}/cm) for separation of the particles over a distance of 4.5 cm between the inlet and outlet ports.

For mixture of the polystyrene particles experiments, a concentration of 1:100 was chosen. Still images of the inlet and outlet ports were captured by fluorescent microscopy at the start of the experiment and of the outlet ports at the end of the experiment and intensity changes noted. Total intensity change was tabulated after the experimental run (3 minutes) at each outlet ports to know the percent of particles travelled to each outlet port. The port having the maximum intensity change for specific wavelength corresponds to accumulation of a particular sized particle. Images were recorded using fluorescent microscopy every 2 seconds

for 30 seconds. This interval time will aid in calculating the particle velocities and deflection from the obstacle, to infer particle trajectories to outlet ports. Based on the separation of these particles in the rectangular, trapezium, and semi-circle designs, the rectangular obstacle geometry was selected for further analysis of the blood samples.

Red Blood Cell Experiments

Whole blood was obtained through venipuncture by trained phlebotomists, drawn into vacutainers (Becton Dickinson) containing 1.8 mg K_2 EDTA per mL of blood, and stored at 4^{o}C in a Biosafety Level 2 refrigerator. 0.25 ml of whole blood sample was taken in a centrifuge vial and diluted to comprise 2 ml of sample volume with 0.14M of phosphate buffer saline (PBS) (0.1 S/m) with initial weight of the sample mixture being recorded. The sample with PBS was mixed thoroughly and centrifuged at 2000 rpm for 5 minutes. The plasma/PBS layer was decanted off and red blood cells were again resuspended in PBS to the same initial weight, mixed and recentrifuged. This process of centrifuging and washing with PBS was conducted three times and the red blood cell mixture at the end of the washing procedure was used for further experiments. This washing procedure was conducted to isolate red blood cell antigen responses in the field from antibody interactions from the plasma. To determine the appropriate dilution of the blood samples, systematic dilution experiments were conducted. Centrifuged red blood cells were diluted using PBS to obtain various concentration levels of 1:60, 1:100, 1:600, and 1:800. Each dilution was loaded into the microdevice separately and imaged using light microscopy. In this experiment for DC dielectrophoresis, the number of red blood cells/ unit area in the field of view is matched to prior data counts of $2.5*10^{-8}$ cells/ μm^2.

Centrifuged red blood cell sample of 1:600 concentration from the dilution experiments were introduced via inlet port to the PDMS microdevice (shown in Figure 4) mounted on Zeiss fluorescent microscope. A DC power supply was used to deliver a range of voltages (10 V-200 V) to determine optimal response of cells. High-resolution video microscopy was used to record bright field video of cell motion and outlet port cell counts within the microdevice.

To determine the total time and the intervals for image collection, systematic experiments will be conducted. The entire experiment will be conducted for total of 15 minutes with each experimental cycle of 3 minutes and 2 second intervals for image collection within the experimental cycle. A total of 3 experimental cycles will be conducted with a gap time of 3 minutes between each experimental cycle. Red blood cell responses to the electric field are slow compared to polystyrene particles and faster imaging speed is not required. Cell movement will be recorded via light microscopy between the insulating obstacle and the bifurcation point. These raw images from the microscope will be used for analysis of velocities of the cells and subsequent travel to the outlet channel. Once the time of experimental run and the interval for image collection is determined, this will be used for further experiments. Cell counts will be tallied in each outlet port at the completion of each run to assess the hypothesis that the port having the maximum cells likely corresponds to a specific blood type. Experiments are run over day 0 (day of collection), 1, 3 and 5 of blood storage for each blood type [16].

Results and Discussions

The quantitative and qualitative analysis of blood types will be demonstrated via DC dielectrophoresis in this work. Here two dependencies will be studied: size dependency via polystyrene experiments and antigen dependency via red blood cell experiments.

Polystyrene Particle Experiments

From size dependency experiments conducted using pure fluorescent polystyrene particles on rectangular obstacle geometry, the authors observed that the 10.35 μm particles deflected closely around the obstacle and preferentially travelled to the lowermost channel (hypothesized O^+ outlet stream in Figure 1) as shown in Figure 5(a) whereas the 5.49 μm particles were not deflected much and travelled into the topmost channel (hypothesized A^+ outlet stream in Figure 1) as shown in Figure 5(b).

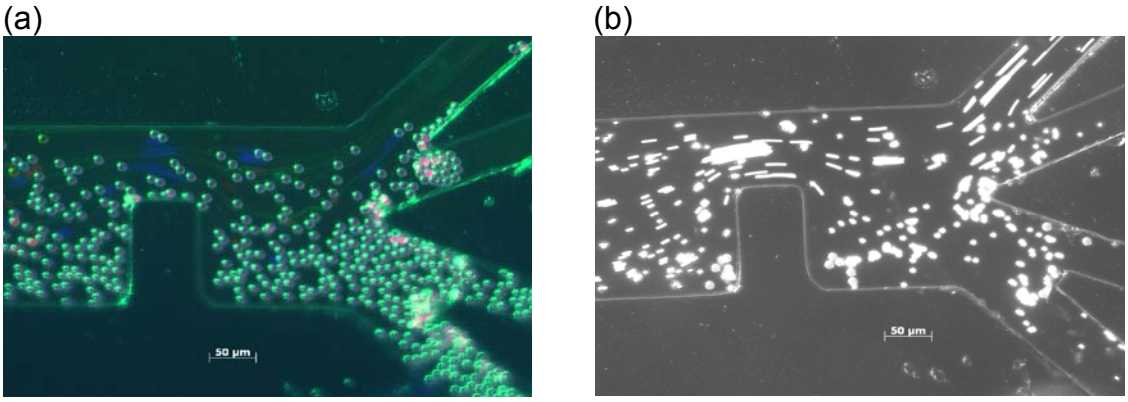

Figure 5: 10.35 μm and 5.49 μm particle trajectories in the rectangular obstacle channel. (a) 10.35 μm particles preferentially flow to channel # 4. (b) 5.49 μm particles preferentially flow to channel # 1.

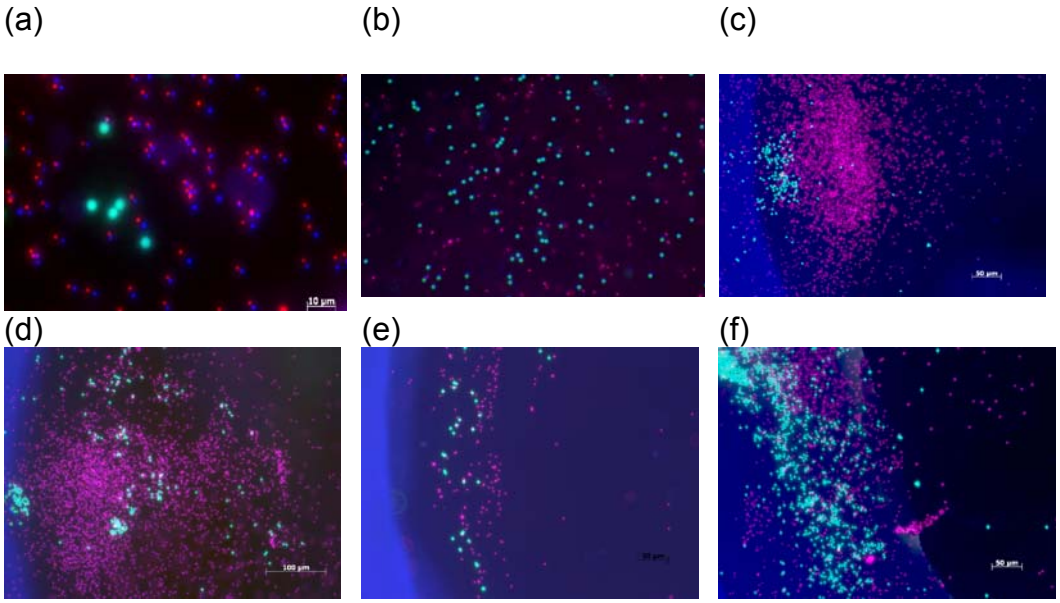

Figure 6: Fluorescent polystyrene particles imaged at the start and end of experimental runs at each ports. (a) Model representing different sizes of polystyrene particles: blue particles are 2.28 μm, dragon red particles are 5.49 μm and green particles are 10.35 μm. (b) Inlet port having all the three sizes of polystyrene particles at the start of the experiment. (c), (d), (e) and (f) Outlet ports 1, 2, 3 and 4 at the end of 3 minute experimental run.

Experiments were also conducted by mixing all the three different diameter polystyrene particles of concentration 1:100 by using 0.14M PBS and are shown in Figure 6 to analyze size dependency. Continuous images were taken for approximately 3 minutes with an interval of 2 seconds. Intensity change will be measured for all the four outlet ports and the port having maximum intensity change for a specific wavelength corresponds to accumulation of a particular polystyrene particle size. The raw images from the microscope will be further analyzed to obtain particle velocities, as an additional indicator to the particle trajectory and subsequent motion into the outlet channels. Figure 6 shows the results of 3 minute experimental run of polystyrene particles. Outlet 1, which is the channel farthest from the base of the rectangular obstacle, has a high concentration of 2.28 μm and 5.49 μm particles (Figure 6(c)) whereas outlet 4 has a high concentration of 10.35 μm particles (Figure 6(f)). Outlet 2 has a high concentration of 5.49 μm particles (Figure 6(d)). This shows that 5.49 μm particles were the least deflected form the insulating obstacle and 10.35 μm particles were the highest deflected which matches with the individual experiment results shown in Figure 5 (a) and (b). Figure 7(a) shows the deflections of the mixture of polystyrene particles from the insulating obstacle into outlet channels. The separation of these particles can be improved by reducing the distance between the electrodes thus creating greater field strength at the obstacle.

Red Blood Cell Experiments

From previous AC-DEP studies by the authors, type A had the largest deflection from high field intensity region whereas type O had the least deflection in the nonuniform electric field. These separations of blood types were achieved in 60 seconds [3]. To achieve a comparable separation in DC-DEP, an intense dielectrophoretic field is necessary. This deflection pattern has been attributed to the existence of antigens on the membrane surface. On this basis, authors are predicting the same pattern of deflection to be followed in DC dielectrophoresis experiments while the blood types separate at the bifurcation point into channels. Images from the microscope will be further analyzed to obtain cell movement. Total cell counts will be tabulated after the entire experimental run to know the percent of cells travelled to each outlet port.

(a) (b)

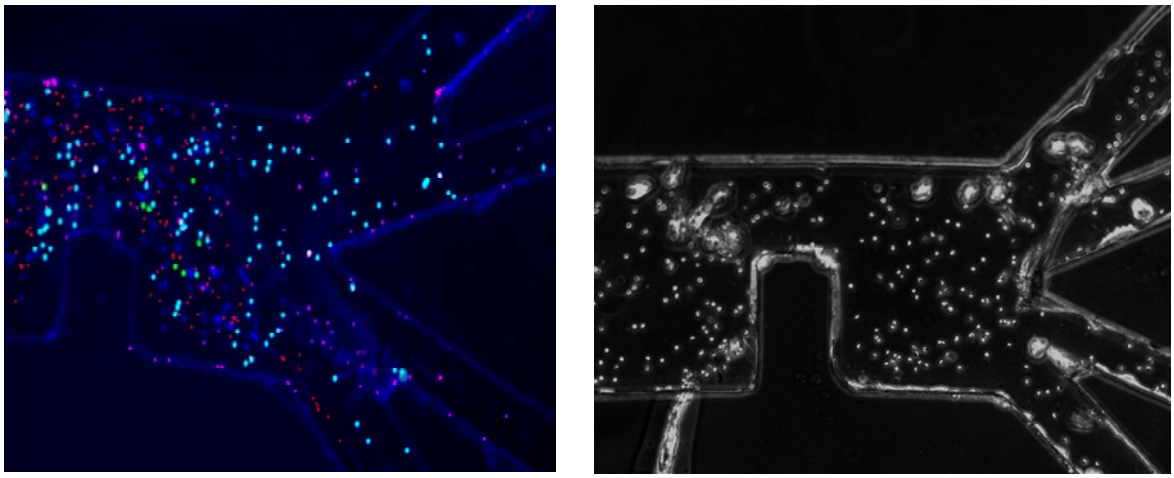

Figure 7: Deflection from the insulating obstacle and particle trajectories for (a) polystyrene particles, and (b) red blood cells.

O^- blood type was introduced into the rectangular geometry-based channel. The authors observed during this experiment that electric field density between the electrodes was not sufficient for separation to occur (Figure 7(b)). The voltage applied through a DC source was 190 V which resulted in electric field strength of 0.00422 V_{pp}/ μm due to the longer distance of 4.5 cm between the electrodes. However, a future design will aid in improving and optimizing device parameters for future experiments; the distance between the inlet and outlet ports (i.e. electrode spacing) has been reduced to 1 cm from 4.5 cm, the distance between channel wall and the obstacle has been reduced to 15 μm, 30 μm and 50 μm from 75 μm and the distance between the insulating obstacle and bifurcation point has been reduced to 50 μm, 75 μm and 100 μm from 250 μm. Thus by optimizing the design parameters we can achieve greater field strength between the obstacle and channel wall thus aiding in reduced separation times compared to AC dielectrophoresis.

Summary

The use of lab-on-a-chip devices for blood typing is a novel technique which will potentially aid in increasing the speed and efficiency of blood type diagnosis. DC dielectrophoresis shows excellent potential for this purpose. Here we have demonstrated separation of erythrocyte responses and polystyrene particles via insulator-based dielectrophoresis. Fabrication of these microdevices was achieved by soft photolithography and PDMS casting. Three geometries (rectangle, semi-circle and trapezium) were assessed for DC dielectrophoretic movement, but the rectangle geometry was selected for further experiments due to better separations achieved during polystyrene particle experiments. From previous research on AC-DEP, four parameters were used to quantify the cell movement based on their blood types: total cell count, vertical movement, horizontal movement and combined distance. The best separation was achieved in 60 seconds with type O being the least deflected and type A being the most deflected from high field density regions [3]. Future work will be to optimize the geometry of the DC-DEP microdevice to achieve similar blood type separations. By optimizing the geometry of the microdevice, the DC voltage applied between the electrodes can be decreased thus increasing the electric field strength between the channel wall and insulating obstacle to maximize electric field density gradients. Increases in electric field density are expected to yield much better separations of blood type erythrocytes. Currently with the rectangular geometry, we have separated 2.28 μm, 5.49 μm and 10.35 μm polystyrene particles at 5 V / 4.5 cm and also have conducted experiments on type O^- red blood cell for optimizing geometry of the device.

References

1. Minerick, A. R. (2008), “DC Dielectrophoresis in Lab-on-a-Chip Devices.” In: Li, Dongqing (ed). *Encyclopedia of Micro- & Nanofluidics*. Springer, Berlin Heidelberg New York (in press).
2. Keshavamurthy S.S., Leonard K.M., Burgess S.C., Minerick A.R. (2008), “Direct current dielectrophoretic characterization of erythrocytes: Positive ABO blood types”, *NSTI-nanotech*, 3, 401–404.

3. Srivastava S.K., Daggolu P.R., Burgess S.C., Minerick A.R. (2008), “Dielectrophoretic characterization of erythrocytes: Positive ABO blood types”, *Electrophoresis*, in press.
4. Minerick, A.R. (2008), "The Rapidly Growing Field of Micro and Nanotechnology to Measure Living Cells," Invited Perspective with Cover Figure, *AIChE Journal*, 54(9), 2230-2237.
5. Lapizco-Encinas B.H., Simmons B.A., Cummings E.B., Fintschenko Y. (2004), “Dielectrophoretic Concentration and Separation of Live and Dead Bacteria in an Array of Insulators”, *Analytical chemistry*, 76, 1571-1579.
6. Kang K, Kang Y, Xuan X, Li D. (2006), “Continuous separation of microparticles by size with Direct current-dielectrophoresis”, *Electrophoresis*, 27, 694-702.
7. Cummings E.B., Singh A.K. (2003), “Dielectrophoresis in microchips containing arrays of insulating posts: Theoretical and experimental results”, *Analytical chemistry*, 75, 4724-4731.
8. Mela P., Van der berg A., Fintschenko Y., Cummings E.B., Kirby B.J. (2005), “The zeta potential of cyclo-olefin polymer microchannels and its effects on insulative (electrodeless) dielectrophoresis particle trapping devices”, *Electrophoresis*, 26, 1792-1799.
9. Barbulovic-Nad I., Xuan X., Lee J.S.H., Li D. (2006), “DC-dielectrophoretic separation of microparticles using an oil droplet obstacle”, *Lab on a chip*, 6, 274-279.
10. Thwar P.K., Linderman J.J., Burns M.A. (2007), “Electrodeless direct current dielectrophoresis using reconfigurable field-shaping oil barriers”, *Electrophoresis*, 28, 4572-4581.
11. Zhang, L.; Tatar, F.; Turmezei, P.; Bastemeijer, J.; Mollinger, J. R.; Piciu, O.; Bossche, A. (2006), “Continuous Electrodeless Dielectrophoretic Separation in a Circular Channel”, *Journal of Physics*, 34, 527-532.
12. Anderson J.R., Chiu D.T., Jackman R.J., Chernlavskaya O., McDonald J.C., Wu H.K., Whitesides S.H., Whitesides G.M. (2000), “Fabrication of topologically complex three-dimensional microfluidic systems in PDMS by rapid prototyping”, *Analytical Chemistry*, 72(14), 3158–3164.
13. Kang, Y.; Li, D.; Kalams, S. A.; Eid, J. E. (2008), “DC-Dielectrophoretic separation of biological cells by size”, *Biomed Microdevices*, 10(2), 243-249.
14. Pysher, M. D., Hayes, M. A. (2007), “Electrophoretic and Dielectrophoretic Field Gradient Technique for Separating Bioparticles”, *Analytical Chemistry*, 79 (12), 4552-4557.
15. Pohl, H. (1978), “*Dielectrophoresis: The behavior of neutral matter in nonuniform electric fields*”, New York, NY, Cambridge University Press.
16. Patenaude S.I., Sato N.O.L., Borisova S.N., Szpacenko A. (2002), “The structural basis for specificity in human ABO(H) blood group biosynthesis”, *Nature structural biology*, 9, 685 – 690.
17. Gasocyne P., Mahidol C., Ruchirawat M., Satayavivad J., Watcharasit P., Becker F.F. (2002), “Microsample preparation by dielectrophoresis: isolation of malaria”, *Lab on a Chip*, 2, 70-75.
18. Gimsa J., Muller T., Schnelle T., Fuhr G. (1996), “Dielectric spectroscopy of single human erythrocytes at physiological ionic strength: dispersion of the cytoplasm”, *Biophys. J.*, 71, 495-506.
19. Daniels G., Bromilow I. 92007), *“Essentials guide to Blood Groups”*, Blackwell Publishing.